

BOOK OF ABSTRACTS

WDS 2026







BOOK OF ABSTRACTS

Week of Doctoral Students 2026

Prague, May 26–28, 2026

© J. Safrankova and J. Pavlu (editors), 2026



CONTENTS

Abstracts are listed alphabetically
by presenting authors in each section.

f-1 Theoretical Physics, Astronomy and Astrophysics	7
f-2 Physics of Plasmas and Ionized Media	12
f-3 Physics of Condensed Matter and Material Research	26
f-4 Biophysics, Chemical and Macromolecular Physics.....	29
f-5 Physics of Surfaces and Interfaces	31
f-6 Quantum Optics and Optoelectronics	35
f-8 Atmospheric Physics, Meteorology and Climatology	36
f-9 Particle and Nuclear Physics.....	37
f-12 Physics Education and General Problems of Physics.....	41
f-13 Physics of Nanostructures and Nanomaterials.....	42



F-1 THEORETICAL PHYSICS, ASTRONOMY AND ASTROPHYSICS

Toward a Complete Hicks Classification of Symmetric Spacetimes


D'Oronzo A. and Málek T.

Abstract. Four-dimensional spacetimes with symmetry are crucial in General Relativity. In 1961, Petrov gave the first classification of them through local group action. In 2016, Hicks refined this classification via Lie algebra–subalgebra (isometry-isotropy) pairs using Schmidt method. This contribution aims to discuss the technicalities of this classification scheme, how the catalogue was built, and present work in progress aiming to fill the final remaining gaps in the list.

Kinetic Study of Shock Formation in Protostellar Jets

Gazdoš J., Araudo A., Tsirou M., and Benáček J.

Abstract. Synchrotron radio emission has been detected from jet termination regions of young stars, indicating the presence of relativistic electrons. Non-thermal electrons are most probably accelerated through the Fermi I acceleration. However, thermal electrons in the jet are not energetic enough to traverse the shock. This brings up the need for an electron pre-acceleration mechanism. We perform Particle-in-Cell (PIC) simulations of these astrophysical shocks.



Kalnajs-Mestel Discs in General Relativity

Hrubeš J. and Semerák O.

Abstract. We describe the Schwarzschild black hole surrounded by a thin disc. The resulting spacetime is axially symmetric and static. First, we obtain a new class of axially symmetric discs by Kelvin transformation of relativistic Kalnajs–Mestel discs. Subsequently, as a superposition of these new discs, we find other discs with vanishing density at their centers, and these can in turn be superposed with a Schwarzschild black hole. The resulting metric is given analytically in closed form. Discs around black holes are often modeled assuming that their matter can be treated as a test one. This is accurate only if the disc’s contribution to the gravitational field is negligible compared with that of the black hole. The advantage of our model is that it can describe more general situations, for example, discs with mass comparable to that of the central black hole.

Impact of Nuclear Star Clusters on the Growth of Supermassive Black Holes

Kománek D. and Wünsch R.

Abstract. The growth of supermassive black holes (SMBHs) requires massive, sustained gas inflows. However, mass transport from 10–100 pc scales remains poorly understood. We investigate how feedback from young massive stars in nuclear star clusters affects mass redistribution in galactic centers. By modeling this stellar feedback as a stochastic process, we present an analytical framework that derives a theoretical prescription for effective viscosity, which scales with the square of the mixing radius.

Unveiling Internal Structure of Contact Binaries

Laversveiler M. and Pejcha O.

Abstract. In low-mass contact binary stars, Thermal Relaxation Oscillations (TROs) are expected to cycle the binaries between contact and semi-detached configurations that, ultimately, merge the object into a single star. We use available data from the Kepler and Gaia missions in order to explore the occurrence of TROs in these systems. Since binaries in our sample show different observational parameters, our goal is to construct a data-driven correction model to observationally constrain TROs occurrence.

Unravelling the Mystery of Intermediate-mass Stellar Mergers

McLachlan D., Carciofi A. C., de Amorim T. H., and Korcakova D.

Abstract. FS CMa stars are a subgroup of stars characterized by forbidden emission lines and the presence of a high abundance of warm dust in their extended circumstellar disks. The origin of such an object remains an open question, but in recent years it has become increasingly likely that FS CMa stars are produced by a merging of low-to-intermediate mass stars. We aim to disentangle the resulting complex circumstellar environment using the radiative transfer code HDUST, as the presence of dust impacts the temperature structure of the disk, the dust and gas components must be modeled simultaneously.

Fast and Reliable Quantum State Tomography

Müller F., Murk S., Tan I., and Šafránek D.

Abstract. Precise knowledge of quantum states is essential for quantum computing, communication, and sensing technologies. However, quantum states cannot be measured directly; they must be inferred from measurement outcomes. Quantum state tomography (QST) reconstructs quantum states from such indirect measurements, in a way broadly analogous to how CT imaging combines multiple two-dimensional projections into a three-dimensional model. The goal of QST is to find the quantum state whose predicted measurement statistics best match the experimentally observed data. This typically leads to a nonlinear optimization problem constrained by the physical requirements that quantum states be positive semidefinite and have unit trace. These are known as the density-matrix constraints. The most common approaches include linear inversion and maximum-likelihood tomography. We discuss how these methods work and highlight their limitations, with the aim of identifying a route toward an optimal tomographic method.



Characterizing Evolved Massive Stars Using Machine Learning

Pandey N., Kourniotis M., and Kraus M.

Abstract. Massive stars beyond the main sequence pose key uncertainties regarding their formation channels, atmospheric processes and mass-loss physics. Towards addressing these points, our work aims to explore machine-learning techniques for characterizing the multiple populations of blue supergiants. We use state-of-the-art expertise on atmospheric modeling and investigate the dynamical wind of these objects and its link to stellar oscillations, which is currently poorly understood.

General Relativistic Effects at the Heart of Sgr A* Light Curve Asymmetry

Rosa V.

Abstract. The supermassive black hole Sgr A*, despite being underluminous, exhibits transient X-ray and near-infrared flares. To understand the physical origin of these rapid variations, it is essential to separate intrinsic emission timescales from relativistic effects, such as Doppler boosting and gravitational lensing, which can complicate the interpretation of flare profiles. This study uses hotspot models to simulate light curves and investigates how parameters like orbital radius, inclination, and intrinsic rise and decay times affect the observed signal. By modeling the intrinsic emission and including relativistic magnification, the study also applies second- and third-moment structure functions to analyze archival X-ray observations, assessing how relativistic effects modify the inferred flare properties.

Probing the Substructure of Galaxy Clusters with Gravitational Lensing

Rowlands Doblas A. D. and Heyrovsky D.

Abstract. We present the current state of the art in gravitational lensing by galaxy clusters. We outline the cosmological motivation of the field and its importance for studying cluster substructure, formed by a system of dark matter halos and subhalos. We discuss current challenges and limitations, focusing on dark matter density profiles, projection effects, and geometrical biases. Finally, we present the numerical framework we are developing to study lensing by increasingly realistic cluster models.

Breakout-type Solar Eruption Observed from Ground and Space

Vávra M. and Dudík J.

Abstract. Among the solar system's most powerful and frequent phenomena are eruptive solar flares. They are caused by magnetic reconnection, during which a sudden change in magnetic connectivity accompanied by energy release takes place. This often results in a coronal mass ejection (CME). Various initiation mechanisms for CMEs have been modeled. One of them is the magnetic breakout model first introduced by Antiochos et al. (1999). They suggest that reconnection progressively removes the overlying magnetic field that restrains a low-lying magnetic flux rope, ultimately allowing it to erupt outward. So far, this configuration has rarely been observed. In this study, however, we identified such a configuration on February 7, 2023, preceding an M1.0-class eruptive flare, as observed by the Atmospheric Imaging Assembly on board the Solar Dynamics Observatory and by our own ground-based H-alpha telescope in Ondřejov.

Conformally Coupled Scalar Field in De Sitter

Voldřich J. and Ortaggio M.

Abstract. We present a study of a system of equations for a conformally coupled scalar field with quartic potential in spacetimes with a cosmological horizon. We will discuss singular points of the system and show how they restrict the existence of the solutions for general initial data. We will show a method that points towards the nonexistence of solutions for a finely tuned coupling constant of the potential outside the two known families of solutions: MTZ and a constant scalar field.

F-2 PHYSICS OF PLASMAS AND IONIZED MEDIA

Evolution of Turbulent Scales Across MHD Shocks

Abushzada L, Pitňa A, Němeček Z., and Šafránková J.

Abstract. Despite decades of study, particle acceleration and turbulent energy cascades in the heliosphere remain under discussion. We use Wind, ACE, DSCOVR and MMS observations to compare turbulence across interplanetary and Earth's bow shocks. Correlation lengths and effective Reynolds numbers are estimated from ACFs. The results highlight upstream–downstream changes, limitations of single-point measurements, and the role of window length in reliable correlation-scale estimates across shock regions.

Characteristics of Charged Particles and Bremsstrahlung Radiation in Laser Foam Interaction at Sub-relativistic Intensity

Agarwal S, Singh S, Devi P, Krupka M, Jelinek S, Dudzak R, Cervenak M, Gajdos P, Novotny J, Mares J, Jaros D, Cikhart J, Cikhartova B, Ettl D, Dostal J, Shelamanov A, Chodukowski T, Rusiniak Z, Zaras-Szydłowska A, Kustos M, Pisarczyk T, Proška J, Sladek J, Krasa J, Krus M, Klimo O, Morace A, and Juha L.

Abstract. Laser-plasma instabilities remain a challenge for efficient energy deposition in inertial confinement fusion. Ultra-low-density foams offer a promising way to enhance absorption and control hot electron generation. At the Prague Asterix Laser System ($\approx 10^{15}$ – 10^{16} W/cm²), we investigated foam targets (ultra-thin SiO₂ shells) using an auxiliary preheating beam (1ω) and main beam (1ω) at varying time delays and characterized the interaction with a suite of complementary diagnostics. In this poster presentation, we show measurements of electron density, hot electron spectra, hard X-ray emission, ion spectra, and electromagnetic pulses, enabling a comprehensive study of charged-particle dynamics and bremsstrahlung in laser-foam interactions at sub-relativistic intensities

Mechanistic Insights into Chlorpyrifos Protonation via $H^+(H_2O)_n$ Clusters

Arepalli N., Jančíšínová A., Matejíček S., and Papp P.

Abstract. To elucidate ion-molecule interactions relevant to ion mobility spectrometry-mass spectrometry, the protonation of chlorpyrifos by hydrated proton clusters ($H^+(H_2O)_{n=3,4}$) was investigated using density functional theory at ω B97X-d/6-311++G(d,p) level of theory. Investigation of proton affinities reveals strong site-selectivity, with pyridinyl nitrogen as the most favorable protonation site, followed by sulfur and oxygen atoms. Thermodynamic results show that proton transfer is feasible only from smaller clusters, whereas larger clusters stabilize the proton and favor adduct formation over direct protonation. Structural analysis indicates notable rearrangements upon protonation. These findings provide molecular-level insight into cluster-assisted protonation mechanisms and support the interpretation of IMS-MS signals.

ACKNOWLEDGEMENT This work was supported by the Slovak Research and Development Agency under the Contract no. APVV-23-0522.

Wave Signatures Upstream and Downstream of Earth's Bow Shock

Balot P., Goncharov O., Šafránková J., Němeček Z., Xirogiannopoulou N., and Grygorov K.

Abstract. Plasma waves play an important role in the interaction between the solar wind and Earth's magnetosphere, particularly in the foreshock and magnetosheath regions surrounding the bow shock. Using multi-spacecraft observations from the MMS mission, we investigate the statistical properties of wave activity in these regions. We further analyze selected events to compare upstream and downstream wave signatures and study how wave characteristics evolve across the bow shock. This combined statistical and event-based approach provides new insight into plasma wave dynamics and shock-related processes in the near-Earth environment.



Ion Emission as a Probe of XUV-induced Damage in ICF First Wall Relevant Refractory Materials

Bulička J., Vyšín L., Medvedev, N., Hájková V., Fekete L., Burian T., Chalupský J., Krása J., Matějčík J., Koch A., Grünert J., Rocca J. J., Menoni C. S., and Juha L.

Abstract. Tungsten, a W/Cr alloy, and pyrolytic boron nitride were ablated with focused 46.9-nm laser pulses (1.5 ns), with the emitted ions analyzed by TOF mass spectrometry. The laser beam fluence at which the ion signal first appears marks the damage threshold: 0.09–0.36 J/cm² for the W samples and 0.78 J/cm² for p-BN, which proves more radiation-tolerant. Unlike morphology-based methods, this ion emission approach works on rough, sintered, or microstructured surfaces typical of real first walls. Threshold values agree with XTANT-3 hybrid code simulations.

Hot Electron Dynamics and Bremsstrahlung Characteristics in Laser-Driven Plasma at PALS

Devi P., Singh S., Agarwal S., Krupka M., Dudzak R., Laso Garcia A., Švandrlík L., Krása J., and Juha L.

Abstract. An optimized filter stack spectrometer (FSS) was developed to measure bremsstrahlung radiation from solid and foam targets irradiated by sub-nanosecond kilojoule-class laser pulses at PALS. Bremsstrahlung diagnostics provide insight into hot electron transport inside the plasma and are compared with electron spectrometer measurements of escaping electrons. Together, both diagnostics enable a more comprehensive understanding of hot electron generation and plasma dynamics.

Ground-Based PWING Observations of Power Line Harmonic Radiation in Finland During Geomagnetic Disturbances

Drastichová K., Němec F., Shiokawa K., and Martinez-Calderon C.

Abstract. Power line harmonic radiation (PLHR) consists of electromagnetic waves generated by power grids at harmonics of the fundamental grid frequency, extending to several kHz. This study analyses PLHR up to 1 kHz using high-resolution wave data from the PWING network in northern Finland (Angeli and Oulujarvi stations). These measurements are compared with nearby IMAGE magnetometer data to examine the link between PLHR and geomagnetically induced currents during space weather events.

Effect of Cold Atmospheric Plasma on Seeds

Fawwaz M. K., Zahoranová A., and Medvecká V.

Abstract. In our work, we studied the effects of plasma produced by diffuse coplanar surface barrier discharge (DCSBD) on pea and radish seeds. The WCA measurements on the seed surface showed a significant decrease in contact angle and improved hydrophilicity in plasma-treated samples compared to the control sample. The germination parameters of plasma-treated seeds were observed for 5 days. Statistical analysis of those parameters shows the dependence of changes on different DCSBD treatments. **ACKNOWLEDGEMENT** This work was supported by the Slovak Research and Development Agency within the project under the contract No. APVV-21-0147 and by the Slovak Grant Agency VEGA No. 1/0366/26.

Dynamics of the Magnetopause During Extreme Conditions: 3-case Study

Ghosh M., Pi G., Šafránková J., and Němeček Z.

Abstract. The dynamics of the magnetopause depend on variations in solar wind conditions. Its expansion and compression, formed due to changes in the dynamic pressure of the solar wind, cause its motions that can be local or global as it moves from one equilibrium state to another. However, the magnetopause itself is not static, as it responds to dynamic fluctuations induced by pressure imbalances and transients, such as the magnetosheath jets. All these dynamic motions are more pronounced during storm events. In the paper, we verify the changes in the magnetopause position for three storms and study their movement in detail.



Dust Particle Impact Detection on Charged Space Probes in the Solar Wind

Houfek P., Souček J., and Santolík O.

Abstract. This paper presents a numerical model designed to simulate dust particle impacts on the surface of a charged spacecraft within the solar wind environment. The modeling process is divided into two stages. In the first stage, the steady-state electrostatic potential around the spacecraft, resulting from interactions with the surrounding plasma, is calculated using the SPIS software. The second stage utilizes these intermediate results as input conditions for a computational model that simulates the expansion of the plasma cloud generated by the dust impact. The model tracks the dynamics of electrons and ions in the vicinity of the spacecraft and calculates the resulting voltage response on the measurement antennas. The results, presented in a 2D approximation, show characteristic signal waveforms and facilitate a better interpretation of data from real space missions.

RF-Induced Evolution of Cavity Transmission in a Trapped-Ion EIT System

Hudák L., Lausti N., Kumar V., and Hejduk M.

Abstract. This work explores the interaction between optical cavity fields and radio-frequency (RF) driven transitions in a trapped Ca^+ ion system using the framework of electromagnetically induced transparency (EIT). A single ion confined in a Paul trap is coupled to an integrated fiber microcavity, and the study focuses primarily on the evolution and dynamics of the intracavity electromagnetic field under external RF excitation. By modeling the probe-field absorption and the cavity response, we investigate how the applied RF signal modifies both the transient and steady-state transmission behavior of the cavity. These effects are examined through frequency-dependent calculations of the cavity transmission spectrum.

Experimental Investigation of Antimony Hall Sensors Under High-fluence Neutron Irradiation

Ivanek M., Duran I., Entler S., Sladek P., Bares O., Soltes J., Viererbl L., Melichar T., Stepan L., Reboun J., Turjanica P., and Bankov R.

Abstract. Magnetic field measurements in fusion reactors require sensors that withstand extreme heat and radiation. Metallic Hall sensors will be used in ITER but DEMO conditions will be more severe. Antimony Hall sensors are being tested under high neutron irradiation in the LVR-15 research reactor. After multiple cycles and high neutron fluence, no significant degradation was observed, confirming their robustness for future fusion diagnostics. This contribution presents the key results obtained so far.

Characterization of Focused Time-delayed Two-color XFEL Beams by Ablation Imprints

Jelinek S., Smid M., Burian T., Vozda V., Vysin L., Hajkova V., Horynova A., Juha L., Vana D., Laso Garcia A., Sripati R., Humphries O., Brambrink E., Appel K., Hoepfner H., Nakatsutsumi M., Andrzejewski M., Bepalov D., Pelka A., Kopecky M., Medvedev N., Zastra U., and Chalupsky J.

Abstract. We characterized a focused two-color two-pulse X-ray laser beam (7060 eV and 7160 eV) utilized in a pump-probe experiment. The pump beam should induce the superionic state in In_2O_3 provided that its fluence exceeds a specific threshold, while the probe beam interacts with both the excited and the non-excited matter. To maximize the probing of the excited state, we characterized the caustics of both beams using the ablation imprint method. Therefore, we determined the fluence distributions for both the pump and probe beams at the optimal probing position.



Design and Development of a 10.6 eV Krypton VUV Lamp for Photoionization in Ion Mobility Spectrometry

Kumar A., Moravský L., Mat'áš E., Kumari P., Ilbeigi V., and Matejčík Š.

Abstract. Ion mobility spectrometry (IMS) separates ions under a uniform electric field. The ionization source is a key element of any IMS instrument. Conventional IMS systems use ^{63}Ni , which is favored due to its long-term stability and operation without an external power supply. Corona discharge (CD) ionization promotes molecular fragmentation, can complicate spectral interpretation. In this work, vacuum-ultraviolet (VUV) photoionization is used to develop an ion mobility spectrometer (IMS). The system employs a 10.6 eV krypton (Kr) discharge lamp as a soft photoionization source. The VUV Kr lamp, powered by a 1.2 kV DC supply, emits radiation at 10.0 and 10.6 eV, enabling efficient ionization of many volatile organic compounds while minimizing fragmentation. The system includes a Kr lamp, VUV window, ionization region, and drift tube, with inlets placed near the lamp for maximum ionization efficiency.

ACKNOWLEDGMENT The work was supported by the Slovak Research and Development Agency under Contract No. APVV-23-0522 and by the Slovak Grant Agency for Science (VEGA 1/0553/22).

Corona Discharge Induced Degradation of 2-Methyl- and 2-Ethyl-2-Oxazoline Studied by Ion Mobility Spectrometry–Mass Spectrometry

Kumari P., Moravský L., Ilbeigi V., Papp P., and Matejčík S.

Abstract. This study investigates the plasma-induced degradation of 2-methyl-2-oxazoline and 2-ethyl-2-oxazoline using a positive corona discharge reactor (CDR) coupled with ion mobility spectrometry–mass spectrometry (IMS–MS). Corona discharge generated reactive species that promoted ring opening, fragmentation, and cluster formation. IMS–MS enabled identification of protonated molecules and degradation products, providing insight into atmospheric-pressure plasma chemistry and oxazoline degradation pathways.

ACKNOWLEDGMENT The studies were funded by the Next Generation EU through the Recovery and Resilience Plan for Slovakia, under project Nos. 09I03-03-V02-00036 and 09I01-03-V04-00025, the Slovak Research and Development Agency under project Nos. APVV-23-0522 and APVV-22-0133 and Slovak Grant Agency VEGA project No. 1/0266/26.

Microfabrication Roadmap for Superconducting Electron-Ion Trap

Lausti N., Kumar V., and Hejduk M.

Abstract We present a roadmap for manufacturing a planar electron-ion Paul trap from a low-loss dielectric substrate (laser-roughened glass [1]) and conductive coating. A high-quality GHz resonator used in electron trapping requires precision down to tens of microns. With a glass substrate, a special manufacturing method is needed to meet the requirements. For this purpose, we apply laser pulses to inscribe circuits in the coating. We form electric transmission lines with the required scale of precision. We also use laser machining for producing through-glass microvias with high circularity. Initial circuit tests confirm high conductance of manufactured circuits.

[1] Antony, A. et al. (2023), Appl. Surf. Sci. 627, 157276

Three-energy-level Ion Structures in Compression Layers: From a Case Study to Multi-event Analysis

Li S., Pi G., Němeček Z., and Šafránková J.

Abstract. We investigated the evolution of magnetospheric boundary layers during the 10 May 2024 ICME-driven shock impact under a northward interplanetary magnetic field (IMF), using coordinated GOES-16 and THEMIS observations. In our case study, we identify a localized compression layer characterized by an enhanced magnetic field and a distinct three-energy-level ion structure, which appears as three separate peaks in the ion energy flux spectra. These peaks are attributed to ions with different mass-to-charge ratios moving with a common bulk velocity, likely associated with plasmaspheric plume transport. To assess whether this structure occurs beyond a single event, we extend the analysis to additional compression layer intervals identified in GOES and THEMIS magnetic field and energy flux data, selected based on strong magnetopause compression (e.g., geostationary magnetopause crossings). The results suggest that this structure is not limited to a single event but may represent an occasional feature formed during rapid magnetopause motion, with potential implications for mass and energy transport across the magnetospheric boundary.



Detection and Analysis of Lightning-generated Whistlers in DEMETER Satellite Data

Linzmayr V., Němec F., Santolík O., and Kolmašová I.

Abstract. We focus on the automated detection of lightning-generated whistlers in DEMETER microsatellite data and on the extraction of their physical parameters. A modified Faster R-CNN framework is used for whistler detection, while a differential evolution algorithm is applied to determine their parameters. Within about 122 days of raw measurements, we identify more than 21 million whistlers. We then analyze the detected events, revealing annual variability and l-shell dependence.

Characterization of Wave Activity in Switchback Boundaries in the Young Solar Wind

Medeiros da Nóbrega G., Dudok de Wit T., Krasnoselskikh V., Alves L. R., and Da Silva L. A.

Abstract. Switchbacks are magnetic structures observed as sudden deflections in the interplanetary magnetic field, which have been occasionally detected along several heliocentric distances over the last decades. With the launch of Parker Solar Probe (PSP) in 2018, the interest in the subject has increased, as measurements in situ have shown that switchbacks are ubiquitously present in the young solar wind, with thousands of events detected on the satellite's first perihelion in November 2018, when it reached a heliocentric distance of around 35.7 solar radii. One of the major open questions regarding switchbacks concerns their boundaries, whether they are permeable or can be eroded, for example, by instabilities. There is now growing evidence that the boundaries are discontinuities of the tangential type. In this study, we focus on wave activity occurring at switchback boundaries and demonstrate their properties. Based on these results, we discuss their impact on the dynamics of switchbacks.

Excitation of Carbon Disulfide by Electron Impact

Megersa G., Garcia E., Bodewits D., Bromley S. J., Stachová B., Matejčík Š., and Országh J.

Abstract. In this contribution, we study electron impact excitation of carbon disulfide (CS_2) using a crossed electron molecular beam method. Electrons with energies from 10 to 100 eV were used. Emission spectra reveal dominant radiation from CS_2^+ molecular ion and CS radical. A 3D spectral electron energy map was constructed. Excitation emission functions and threshold energies were determined. The results provide new reference data and insight into electron induced processes in CS_2 .

Pulsed Bias Effects on SnO_2 Thin Films Deposited by ECWR Plasma

Mekki R. N., Mašek T., Čada M., Kudrna P., Tichý M., and Hubička Z.

Abstract. Tin oxide (SnO_2) thin films deposited via Electron Cyclotron Wave Resonance (ECWR), offer precise control over film properties for advanced optoelectronic and sensor applications. These studies examine how varying substrate bias during ECWR deposition influences SnO_2 film characteristics, including crystallinity, electrical conductivity, optical properties, and thickness. We are studying to confirm that bias-driven plasma density modulation optimizes oxide film uniformity and stoichiometry, with pulsed modes further stabilizing discharge parameters to achieve deposition rates exceeding 15 nm/s for scalable, industrial production. We are investigating the deposition pulse-optimized ECWR SnO_2 films as superior alternatives to ITO in flexible electronics, thereby advancing energy-efficient, low-temperature deposition processes suitable for roll-to-roll manufacturing and sustainable device fabrication.



STAT-TS Dataset from January 2022 to May 2025

Mičko L., Souček J., Píša D., and Santolík O.

Abstract. Onboard Solar Orbiter spacecraft, RPW-TDS instrument provides data related to plasma waves and dust events. We attempt to use these data to build a new STAT-TS dataset based on two main products of the instrument, the triggered waveform snapshot dataset (TSWF), containing whole waveform snapshots, and the statistical dataset (STAT) made of basic information about all RPW-TDS recorded events. In our work, we focus on wave events and aim to identify waves as Langmuir waves or ion acoustic waves, and to better understand their statistical properties by assessing several related data relationships such as wave event counts over time or distance, polarization coefficient relation to the electric field amplitude of waves, or solar wind speed measured at observed wave events over the entire span of the Solar Orbiter mission. In the current STAT-TS version, we cover data from 1st January 2022 to 31st May 2025.

Influence of Magnetron Sputtering Type on the Properties of ZrO₂ Thin Films

Naiko L., Hippler R., Wullf H., Helm C. A., Wallis J., Kruth A., Chvostova D., Olejnicek J., Cada M., and Hubicka Z.

Abstract. Zirconium dioxide thin films were deposited at various substrate temperatures using high-power impulse magnetron sputtering (HiPIMS) and radio frequency (RF) magnetron sputtering techniques. The structural and optical properties of the deposited films were investigated by X-ray diffraction (XRD), Raman spectroscopy, and spectroscopic ellipsometry. XRD analysis confirmed that the ZrO₂ films had formed in a monoclinic phase. Spectroscopic ellipsometry measurements revealed the ultra-wide band gap nature of the deposited zirconia coatings.

Energy Emitted by Jovian Lightning Step Leaders

Rosická K., Kolmašová I., Santolík O., Imai M., and Píša D.

Abstract. The lightning development process consists of multiple stages. Studying this process on Jupiter requires spacecraft measurements with sufficient temporal resolution, provided by the Juno Waves instrument detecting lightning-generated whistlers. Groups of whistlers were previously interpreted as signals generated by in-cloud lightning leaders. We calculated Poynting flux for individual whistlers within each group and found that the distribution of their energies does not show any general trend.

Characterization of a Novel FEBID/FIBID Precursor Molecule

Saha S., Das S., Lyshchuk H., Kočíšek J., Fedor J., and Nag P.

Abstract. We studied electron/ion beam-induced dissociation of iron tetracarbonyl acrolein, $\text{Fe}(\text{CO})_4(\text{CH}_2=\text{CHCHO})$, a potential FEBID and FIBID precursor molecule[1]. Anionic fragments formed via dissociative electron attachment (DEA) were investigated using low-energy electrons(0–12 eV), while cationic fragments were studied at 70 eV. Electron-induced processes were studied using two complementary setups at the Heyrovský Institute, a trochoidal electron monochromator with a quadrupole mass spectrometer (TEM-QMS)[2], the CLUster Beam (CLUB)[3] apparatus. Ion beam induced processes were studied using the ARIBE, low energy ion facility at GANIL[4], Caen, France. Fragmentation products were measured for He^+ , Ne^+ and Ne^{4+} projectiles with incident energies 16, 6 and 40 keV, respectively.
1.S. Das et al., J. Phys. B 59 035201(2026);
2.J. Langer et al., Eur. Phys. J. D, 72, 112 (2018);
3.M. Fárník et al., Phys. Chem. Chem. Phys. 23, 3194(2021);
4.V. Bernigaud et al., Publ. Astron. Obs. Belgr. 84, 83–86 (2008).



Kinetic Modelling of H_3O^+ Ion Formation at Low Temperature

Slezak P., Van Houten S., Dohnal P., Rednyk D., Plašil R., Roučka Š., and Glosik J.

Abstract. The formation of H_3O^+ ions at low temperature is investigated using a chemical kinetics model of an afterglow plasma. The main aim of the model is to describe the ion-molecule chemistry that can lead to H_3O^+ becoming the dominant positive ion under the studied experimental conditions. The work focuses on identifying the reaction pathways that control the production and loss of hydronium, and on understanding how competing oxygen and hydrogen containing ions influence its abundance.

Processing of Ion VDFs from the SPAN-I Measurement Onboard Parker Solar Probe

Sruti Satyasmita, Ďurovcová T., Němeček Z., and Šafránková J.

Abstract. The origin of the proton beam, a secondary proton population observed in the solar wind, remains unclear. Data from SPC instrument onboard Parker Solar Probe (PSP), and earlier observations from the Helios mission, suggest that the relative proton beam abundance increases from the Sun to Earth. In addition to the SPC, the PSP is equipped with the SPAN-I instrument, which measures ion velocity distribution functions (VDFs) during the PSP's perihelia that are not covered by the SPC instrument. However, the limited field of view of the SPAN-I instrument prevents direct observation of the full ion VDFs. We apply the Gyrotropic Slepian Reconstruction method (Das and Terres, 2025b) to recover the full proton VDFs and perform bi-Maxwellian fitting to derive the parameters of the various populations. We observe that the proton VDFs often have three populations: a dominant proton core and two proton beams. The drift velocity of the secondary beam remains close to the local Alfvén speed. This suggests that the formation of the beams may be related to reconnection processes near the Sun. Thus, we focus on variations of the proton beam parameters across switchbacks that could be remnants of reconnection.

Investigation of Plasma–Material Interactions on Different Substrates Using a Hot Tungsten Cathode System for Liquid Metal Divertor Applications

Turek Z., Mašek T., Mishra H., Mekki R. N., Čada M., Hubička Z., Tichý M., and Kudrna P.

Abstract. We present a hot tungsten cathode system to study the interactions between low-temperature plasma and thin metal layers sputtered onto both conductive and non-conductive substrates. This research aims to understand material selection for liquid metal divertor applications.

Collisional Quenching of Vibrationally Excited H_3^+ Ions

Van Houten S., Rednyk D., Dohnal P., Roucka S., Plasil R., and Glosik J.

Abstract. A radiofrequency 22-pole trap apparatus is used to determine quenching rates for vibrationally excited H_3^+ ions employing laser-induced reaction (LIR) schemes and leak-out spectroscopy (LOS). The quenching process represents collisional cooling of excited species using a non-reacting gas. The H_3^+ ion is among the most abundantly produced ions in the interstellar medium, and it was observed in a variety of environments, such as dense and diffuse molecular clouds, ionospheres of gas giants, and towards the Galactic Center. For the LIR (LOS) method, the reaction rate coefficients for the collisional quenching of the ion vibrational excitation are inferred from the dependence of the measured ratio of secondary (leaked) to primary ions on the density of the collisional partner.

Investigation of the Inverse Plasma Sheath via BIT1 PIC Modeling

Vrba Š., Tskhakaya D., and Komm M.

Abstract. In a classical plasma sheath, the potential decreases from the upstream towards the wall. The absolute value of the potential drop depends on a number of parameters, such as the electron temperature and the flux of electrons emitted from the surface. The question then is whether the wall potential can ever exceed the plasma potential – whether there is a realistic access to the so-called inverse sheath in tokamaks. We start our investigation from the work of Campanell and Umansky, reproduce their regime, and determine whether it is applicable to fusion-relevant conditions. Afterward, we explore the theoretical conditions for accessing the inverse sheath.



F-3 PHYSICS OF CONDENSED MATTER AND MATERIAL RESEARCH

Structural (In)Stabilities in Rare-Earth $A_2B_2O_7$ Oxides

Hájek F., Staško D., and Klicpera M.

Abstract. $A_2B_2O_7$ oxides ($A = \text{Sc, Y, La-Lu}$; $B = \text{p or d-element}$) form a broad family of materials exhibiting often complex electronic, magnetic, and material properties, resulting in diverse potential applications. The geometrically frustrated lattices, spin-orbit coupling, and exchange interactions give rise to diverse emergent conducting and magnetic states. Moreover, by introducing dopants, the crystal lattice and derived behavior could change significantly, allowing a fine-tuning of specific properties. Our work focuses on magnetism of the $A_2\text{Ir}_2\text{O}_7$ series and on the local structure in the substituted $A_2(\text{Ti,Zr})_2\text{O}_7$ series.

Ergotropy Extraction Under Observational Constraint

Hochmann V. and Šafránek D.

Abstract. Ergotropy quantifies the maximum work that can be extracted from a quantum state by unitary operations. We study ergotropy extraction when the state is not fully known, and only coarse-grained measurements on many identical copies are available. We present a protocol for work extraction under such observational constraints and discuss its possible implementation on a trapped ion quantum simulator.

Energy Landscape of Perovskites Using the VASP Force Field and GRACE Foundation Models

Khanore M., Klic A., and Marton P.

Abstract. The energy landscape is essential for material investigations, but using first-principles methods can be computationally intensive. Researchers have traditionally addressed this through empirical potentials such as the Shell model, effective Hamiltonians, and Landau theory. Recently, machine learning interatomic potentials (MLIPs) have emerged as a viable alternative, offering accuracy comparable to that of density functional theory (DFT). In this study, we examined two methods: the Vienna Ab initio Simulation Package machine-learned force fields (VASP MLFF) and the Graph Atomic Cluster Expansion (GRACE) foundation MLIP, both with and without fine-tuning, for PbTiO_3 , BaTiO_3 , and CaTiO_3 perovskites. We tested it on datasets generated with a 40-atom supercell in ab initio molecular dynamics, heated from 1 K to near the Curie temperature. Our findings show that fine-tuning the GRACE MLIP on high-quality data can match DFT accuracy for forces and energy. Furthermore, we conducted molecular dynamics simulations of a 1,080-atom PbTiO_3 supercell and verified the fine-tuned model's ability to capture phase transitions.

Defects and Strain Engineering in Non-collinear Antiferromagnet

Machacova N. and Carva K.

Abstract. We study the non-collinear antiferromagnet Mn_3NiN using first-principles calculations. To model realistic thin films, we first determine how biaxial strain affects the magnetic ground state. We further show that line defects arising from a mismatched substrate break local symmetry and induce a finite magnetization. The results are of interest to the antiferromagnetic spintronics owing to the small stray fields and fast magnetization dynamics.



Polarized Optical Spectroscopies of NdFeO₃

Michal O., Moreira J. A., Dronova M., Verseils M., Brodavka F., Nguyen H. D., Miranda A., Silva A., Lebeda M., Nužnyj D., Mihalik M., and Kamba S.

Abstract. Using polarized IR spectroscopy, we focus on the spin-reorientation transition (SRT) in NdFeO₃ between 170 K and 110 K, driven by the interaction of the Fe and Nd magnetic sublattices. Both above and below the SRT, the structure is described as orthorhombic. The reorientation, however, raises symmetry arguments in favor of a monoclinic symmetry-lowering. Surprisingly, there hasn't been any direct experimental proof yet. For that reason, we present the temperature- and pressure-dependent evolution of polarized IR spectra, which should reveal any signs of a structural transition.

Corrosion Behavior of Additively Manufactured WE43 Magnesium Alloy: Influence of Surface Condition and Lattice Geometry

Nazarenko D., Alomar Z., D'Elia F., Dobroň P., and Drozdenko D.

Abstract. The aim of this study is to investigate the corrosion behavior of powder bed fusion-manufactured WE43 magnesium alloy by combining potentiodynamic polarization testing with in situ acoustic emission monitoring. For bulk WE43 specimens, the electrochemical response was strongly dependent on the initial surface state. For printed lattice structures, geometry strongly influences corrosion behavior.

Cohesive Zone Modeling of Interfacial Damage Evolution in Aluminum–Stainless Steel Bimetallic Laminates Under Cyclic Compressive Loading

Ravikumar C. and Šlapáková M.

Abstract. This study investigates progressive interfacial delamination in aluminum–UNS N08031 stainless steel laminates under cyclic compressive loading using Cohesive Zone Modeling (CZM). Results revealed stress concentrations up to 600 MPa, irreversible interface damage, and ±40 MPa shear stresses driving mixed-mode debonding. The work supports durability assessment and interface optimization for heat exchangers, marine systems, and corrosive industrial structures.

F-4 BIOPHYSICS, CHEMICAL AND MACROMOLECULAR PHYSICS

Probing Transmembrane Protein Nano-environment Using FRET-GP

Hodoš M. and Pokorná Š.

Abstract. Transmembrane proteins (TMPs) embedded in the lipid bilayer facilitate crucial processes in cells. Growing evidence shows that TMPs' function is affected by the lipid packing of the membrane in their proximity.[1] To probe the TMP nano-environment, we combine FRET and GP approaches. By developing and validating a combined FRET-GP approach for live cell application, we aim to provide insights into the transmembrane protein regulation by their lipid nano-environment in physiologically relevant conditions.

[1] Levental, I. et al. Nat. Rev. Mol. Cell Biol. 24, 107 (2023)

Fifth-order Pump-probe Spectroscopy

Charvatova K., Bruschi M., and Maly P.

Abstract. Conventional third-order pump-probe spectroscopy cannot directly resolve exciton transport in nearly isoenergetic molecular systems. We study fifth-order pump-probe signals sensitive to exciton diffusion and exciton-exciton annihilation. Using a theoretical model with realistic spectral lineshapes, we show that spectrally resolved signals provide detailed information about molecular structure that is inaccessible from the spectrally integrated signals studied so far.

Resistive Switching in Nanofluidic Systems for Neuromorphic Applications

Katuta R., Wahid I., Červenková V., Nikitin D., and Choukourov A.

Abstract. Neuromorphic computing requires hardware elements that can mimic synaptic plasticity. While solid-state devices are widely studied, fluidic systems offer unique advantages. This work investigates the resistive switching properties of nanofluids prepared by loading gas-phase aggregation metal nanoparticles into liquid polymers. The use of various nanoparticles and polymers enables the development of nanofluidic systems as a potential platform for neuromorphic hardware.



Negative Staining of Lipids within Living-cells by Lanthanide-based Raman Tags

Tong X., Pelc R., Mojzeš P., and Wu T.

Abstract. Lanthanide complexes are well known for their sharp luminescence and wide applications in biosensing, bioimaging, and material science. Among them, the water-soluble $[\text{Eu}(\text{DPA})_3]^{3-}$ complex (DPA = 2,6-pyridine-dicarboxylic acid) exhibits intense and narrow emission bands—particularly the hypersensitive $5D_0 \rightarrow 7F_2$ transition 615 nm, it appears at $\approx 2545 \text{ cm}^{-1}$ in Raman under 532 nm excitation. These luminescence bands lie outside the typical Raman region of biomolecules, enabling simultaneous detection of Raman and luminescent signals for enhanced image contrast.

Cancer Biomarker Detection: Combining Antifouling Surfaces and DNA Nanostructures for miRNA Sensing

Vogelová E., Hovanová V., Hansen N., Petráková V., Šulc P., and Lísalová H.

Abstract. MicroRNAs (miRNAs) serve as biomarkers for various diseases, including cancer. However, their detection often relies on traditional methods, which usually struggle in complex media and require lengthy sample pretreatment. We approached miRNA sensing by integrating antifouling zwitterionic polymer brushes with DNA nanostructures. Using surface plasmon resonance (SPR), this platform enables real-time direct detection of miRNA at nanomolar level in 50% human blood plasma with minimal pretreatment.

Phase and Morphological Tuning of Iron Nitride Nanoparticles via Reactive Cylindrical Magnetron Sputtering

Wahid L., Katuta R., Červenková V., Nikitin D., and Choukourov A.

Abstract. Fe_xN nanoparticles (NPs) show potential for sustainable technologies, but controlling their phase and morphology is challenging. This work presents a one-step, solvent-free synthesis method using a gas-aggregation-cluster source with a cylindrical magnetron. Varying N_2 content in the gas phase drives transitions from metallic Fe to various Fe_xN phases. These results improve the understanding of the properties of Fe_xN NPs and support their prospective application in advanced functional materials.

F-5 PHYSICS OF SURFACES AND INTERFACES

Development of Electrochemical Characterization Techniques for Hydrogen Evolution Reaction Directly in Operating Water Electrolyzer

Herman J., Hrbek T., Kůš P., and Matolínová I.

Abstract. Electrochemical impedance spectroscopy combined with the distribution of relaxation times enables the separation of individual contributions to overall losses in a water electrolyzer. Thin-film sputtered platinum catalyst reveals two well-distinguishable processes attributed to anodic and cathodic reactions, which are sensitive to local hydrogen and oxygen concentration. Together with the implementation of a reference electrode, a valuable insight is gained for operando electrolyzer characterization.

Model Pt–Ru Surfaces Under AEMFC Relevant Conditions: A NAP-XPS Study

Chakraborty S., Oveysipoor S., Dínková T.N., Vorochta M., and Matolínová I.

Abstract. Understanding catalytic processes at the anode of Anion Exchange Membrane Fuel Cells (AEMFCs) is essential for improving both performance and durability. Although Platinum (Pt) remains the benchmark catalyst, its HOR (Hydrogen Oxidation Reaction) kinetics in alkaline media are sluggish. Alloying Pt with Ru has been shown to improve the HOR performance of Pt-based catalysts; however, the precise mechanism behind this enhancement is still under investigation. In this study, we investigated the role of Ru by examining three model catalyst surfaces: pure Pt, pure Ru, and a Pt–Ru bimetallic system. Using Near Ambient Pressure X-ray Photoelectron Spectroscopy (NAP-XPS), we investigate the chemical and electronic changes at the anode surface under water exposure, which simulates realistic fuel cell conditions. On the Pt surface, we observe a single type of hydroxide species. In contrast, the Pt–Ru surface exhibits an additional OH feature, suggesting a distinct interaction involving both Pt and Ru. These surface modifications indicate changes in the interfacial behavior of hydroxide species, which may influence the accessibility of reaction-relevant sites.



Characterization of Platinum Catalysts with Reduced Pt Loading

Kalabis D., Yakovlev Y., Lobko E., Kalinovych V., Tsud N., and Rodriguez M.

Abstract. Electroless deposition was used to prepare platinum catalysts with ultralow Pt loading on Au substrates. A sacrificial Cu layer is first electrochemically deposited and subsequently replaced by Pt via redox reactions. XPS confirmed sub-nanometre Pt layers ($\approx 1\text{--}3 \mu\text{g}/\text{cm}^2$). Electrochemical tests show increasing catalyst activity, demonstrating a cost-effective route to efficient Pt catalysts.

Pressure-dependent CO Adsorption and Electric-field-induced Surface Restructuring of Ni(111) Studied by Near-Ambient Pressure STM

Ormoš M., Oveysipoor S., Matvija P., and Matolínová I.

Abstract. CO adsorption on Ni catalysts is central to the Fischer–Tropsch process, yet adsorption sites remain debated. We investigate dense CO layers on Ni(111) from UHV to 50 mbar using near-ambient-pressure STM. We determine pressure-dependent coverages up to 0.77 ML and resolve their structures, including new phases at higher pressures. Above 1 mbar, electric field effects induce Ni restructuring, likely via Ni carbonyl species, which is relevant for CO-rich environments in electrocatalysis.

Dynamic Redistributing of Fe Within the CeO₂ Model Catalysts Under Reducing and Oxidizing Conditions

Pchálek F., Oveysipoor S., Matvija P., and Matolínová I.

Abstract. Transition metal modification of CeO₂ enhances catalytic activity, however, the dopant redistribution under reaction conditions is often overlooked. Using Fe–CeO₂ as a well-defined model system, we show that Fe migrates from the surface to the bulk under reducing atmospheres, while oxidizing conditions stabilize it at the surface. Combining STM, XPS, depth profiling, and NAP experiments, we clarify the Fe localization, reversibility of the process and its impact on catalytic performance.

Develop a Catalyst for Anion Exchange Membrane Fuel Cell

Vyshak D. R. and Yakovlev Y.

Abstract. Our study focuses on the synthesis and electrochemical study of Mxene for Potential electrocatalyst application for AEMFC. Mxene, a class 2D metal carbide, has attracted attention due to its electroconductivity and large surface area. These properties make Mxene an excellent support material. In the present work, Mxene was synthesized through selective etching, and its electrochemical properties were studied. The prepared Mxene material exhibits a layered sheet-like structure with a high density of exposed active sites, which enhances electrochemical reactions. The high conductivity and surface functionality of Mxene contributed significantly to the improved electrochemical performance of the synthesized material. Electrochemical measurements were carried out using CV and Cdl analysis. Cv measurement within the potential range of -0.9 V to -0.3 V at different scan rates. Overall, this study highlights the potential of Mxene as a promising material for electrocatalytic and fuel cell applications.

Temperature and Electric Field Dependent Migration of Polarons in Hematite Fe_2O_3

Sreekumar S., Caldentey L. A., Alexander A., Redondo J., Tobisch S., Kocan P., Riva M., and Setvin M.

Abstract. The non-contact atomic force microscopy (nc-AFM) technique has recently enabled precise manipulation of single charges. In this work, we exploit this capability to investigate polaron dynamics at the single-quasiparticle limit. Polarons are self-localized charge carriers arising from strong electron-lattice interactions in ionic crystals and they play a central role in determining key material properties, including conductivity, catalytic activity, and emergent phenomena such as high-temperature superconductivity and colossal magnetoresistance. This work presents a methodology for controlled charge injection, localization, and quantification on insulating surfaces, enabling direct investigation of polaron behavior in hematite (Fe_2O_3). Systematic experiments performed under varying tip-sample conditions demonstrate how mobility depends on the local electric field and temperature, establishing a pathway for quantitatively probing polaron transport at the atomic scale.



Structure and Thermal Stability of Ce-modified $\text{Co}_3\text{O}_4(111)$ Surfaces

Škvára J., Petrov S., Johánek V., and Mysliveček J.

Abstract. Metal-oxide-based nanostructures have the potential to become accessible, efficient, and stable catalysts for future applications in energy storage. In particular, the Ce/ CoO_x structure is significant for its thermal stability and its catalytic activity towards redox reactions. In the present study, we characterized the Ce/ CoO_x structure by means of X-ray photoelectron spectroscopy (XPS), energy-dependent low energy electron diffraction (IV-LEED) and scanning tunneling microscopy (STM) over temperature range from 323 K to 923 K. We identified three temperature intervals with distinct behaviors of various structural properties. In the interval from 323 K to 473 K the Ce/ Co_3O_4 system is thermally stable, and the Ce layer is amorphous. Between 473 K and 773 K the Ce forms an ordered structure and gradually becomes partially oxidized as CeO_x upon annealing, while the system is still stable. In the last interval, above 773 K, the spinel structure begins to collapse, the CeO_x becomes fully oxidized, and the Co_3O_4 is gradually reduced.

F-6 QUANTUM OPTICS AND OPTOELECTRONICS

Terahertz Spectroscopy of Plasmons in Arrays of Graphene Dots and Holes

Matuška R., Němec H., Kunc J., Klusáková B., Singh A., and Kužel P.

Abstract. Ultrabroadband THz spectroscopy (0.3–16 THz), a powerful tool for characterization of thin films, nanostructures, and 2D crystals, was used to study plasmonic response and ultrafast conductivity dynamics in quasi-freestanding single-layer graphene grown on SiC. Graphene dots and holes patterned into square and hexagonal lattices were characterized by THz time-domain spectroscopy, optical pump–THz probe measurements resolving sub-picosecond photoconductivity evolution, and complementary THz-SNOM imaging.

Heat Load in Gain Fibers — Transverse Mode Instability

Slechtsa M.

Abstract. Transverse Mode Instability (TMI), induced by dynamic nonlinear stimulated thermo-optical scattering process, invokes deterioration of beam quality and average power, and becomes the primary limitation to power scaling in high-power fiber lasers and amplifiers. We introduce the theoretical description of the effect incorporating the formation of modal interference pattern (MIP) that induces the refractive-index grating (RIG) and the origin of the phase shift between them, furthermore the experimental observations and suggestions for suppressing the TMI in confined-doped fibers.



F-8 ATMOSPHERIC PHYSICS, METEOROLOGY AND CLIMATOLOGY

Enhanced Impact of BVOC Emissions on Near-Surface Ozone over Central Europe: Analysis of the Meteorological and Chemical Drivers

Jadhav H. and Huszár P.

Abstract. Ozone (O_3) presents a paradox in atmospheric chemistry: stratospheric ozone shields the Earth from harmful ultraviolet radiation, whereas elevated tropospheric ozone, formed by complex reactions of volatile organic compounds (VOC) with nitrogen oxides, acts as a secondary pollutant linked to adverse health and ecosystem impacts across Europe. Using a 10-year chemistry transport model (CAMx) simulation, this study investigates the chemical and meteorological controls governing the ozone formation driven by VOC of biogenic origin (BVOC), focusing on the extremes of the BVOC impact. Results indicate that 2 m temperature alone modulates BVOC impacts more strongly than synoptic circulation types, while the highest BVOC impacts occur not only in NO_x -limited regimes but also primarily under VOC-limited and transitional regimes over urban city centers.

Validation of LES Turbulence and Air Quality Simulations Using Wind Tunnel Model Measurements

Rizziero F., Fuka V., Geletic J., Resler J., Reznicek H., Jacubcová M., Nosek Š., Belda M., and Krč P.

Abstract. The Microbus project aims to evaluate the effect of traffic scenarios on the city of Prague in terms of air quality. Particularly relevant is the urban hotspot of Legerova Street, an area highly exposed to heavy urban traffic, which is reproduced with realistic flow fields and pollutant concentrations using a wind tunnel model. In this study, the measurements are then compared with outputs from three LES models. Validation of microscale models against the Microbus experimental results is essential for assessing the models' ability to replicate realistic air quality conditions.

F-9 PARTICLE AND NUCLEAR PHYSICS

Prague's Contribution to the ATLAS Inner Tracker Upgrade

Bucko J.

Abstract. The LHC will undergo a major upgrade during the upcoming Long Shutdown 3. The goal of the upgrade is to increase the collider luminosity, i.e. the number of collisions per second. This means higher strain on the already aging ATLAS detector, so it also has to be upgraded. Part of the upgrade is replacement of the current tracker for new full-silicon tracker called Inner Tracker (ITk). This poster describes the process of manufacturing and testing the ITk modules as it is done here in Prague.

Direct and Indirect Dark Matter Searches at the COMPASS and AMBER

Dehpour M.

Abstract. This presentation outlines my Ph.D. research on Dark Matter (DM) searches using CERN's COMPASS and AMBER experiments. At AMBER, I measure hadron production to reduce systematic uncertainties in astrophysical antiproton backgrounds, vital for indirect DM searches by AMS. Parallely, I investigate direct DM production signatures at COMPASS. Together, these complementary approaches bridge experimental data with cosmological models to constrain the dark sector.



Pairing Properties of Finite Nuclei from Realistic Nuclear Interaction Models

Folprecht R. and Knapp F.

Abstract. Nuclear pairing, also commonly referred to as nuclear superfluidity, is a well-established concept of nuclear many-body physics. It plays a crucial role in a wide range of nuclear phenomena, including nucleon separation energies, the structure of low-lying excited states, and the enhancement of nuclear transition rates. To date, however, the vast majority of the theoretical predictions concerning the nuclear pairing effects remain deeply rooted in phenomenological schematic models or density functional theory calculations. In the present contribution, we systematically study and evaluate the ground-state properties of selected isotopic chains of even-even nuclei with emphasis on the analysis of the pairing properties. To this end, we employ the Hartree–Fock–Bogoliubov quasiparticle mean-field method and the Lipkin–Nogami extension thereof as well as the beyond-mean-field symmetry-broken Bogoliubov Many-Body Perturbation Theory using nuclear interaction models derived from chiral effective field theory.

Calibration of the ATLAS Tile Calorimeter Using Minimum Bias Currents

Haviernik M.

Abstract. The Tile Calorimeter (TileCal) at the ATLAS detector captures hadronic products of particle collisions at LHC and measures their energy using scintillating tiles as active material. The response of TileCal varies over time due to radiation exposure during data taking. Stability of response is monitored by dedicated calibration methods, one of them being Minimum Bias calibration. This work presents Run 3 Minimum Bias calibration results, showing response variation of select Tile regions.

169-Tm(n, gamma) Cross Section and Statistical Gamma Decay Properties from DANCE Measurements

Knapová I., Horčíčková K., Couture A., Fry C., Prokop C., Cidoncha E. L., Gusing F., Rusev G., Ullmann J., Kelly K., Krticka M., Reifarth R., Valenta S., and Kawano T.

Abstract. We report new measurements of the $^{169}\text{Tm}(n,\gamma)$ cross section and statistical gamma decay of ^{170}Tm using DANCE detector at LANSCE [1]. The cross section was determined from 1.8 eV to 0.97 MeV, revealing eight new resonances. The statistical gamma decay of ^{170}Tm was investigated utilizing DICEBOX algorithm; scissors mode was identified at 3.3 MeV. The revised data increase the predicted s-process abundance of ^{169}Tm by 26 %.

[1] I. Knapova, K. Horcickova et al., Phys. Rev. C 112 (2025) 014612

Study of the Double Dalitz Decay of Neutral Pion at NA62 Experiment

Lelák M.

Abstract. Studies of rare neutral-pion decays, such as the double-Dalitz decay into two electron-positron pairs, provide an important input to the theoretical modeling of the form factor that describes decays and interactions of neutral pions. The NA62 experiment at CERN has collected a large dataset of charged kaon decays with electron-positron pairs in the final state since 2017. The goal of this work is to analyze the NA62 data and perform a measurement of the branching fraction of the double-Dalitz decay of the neutral pion and improve the precision reached by other experiments.

RICH Performance and Particle Identification Studies for COMPASS SIDIS

Pucci P.

Abstract. The presentation focuses on analyses conducted on a RICH detector used in COMPASS, a fixed target experiment, for processes like Semi Inelastic Deep Inelastic Scattering. The first part is dedicated to the detector's measurement stability, while the second focuses on measured data of known decays so as to analyze the identification efficiency of particles relevant for the scattering (pions, kaons, and protons).



Investigation of Top–Antitop Quark Production at the LHC

Samara D.

Abstract. The large mass of the top quark makes it a fascinating particle for precision studies of the Standard Model (SM) and for searches for possible effects beyond the SM. The Large Hadron Collider provides an unprecedented number of proton-proton (p-p) collisions where the top-quark production can be tested. In particular, the measurement of the charge asymmetry in top-antitop quark production is an important test of the SM and can reveal new phenomena. This talk will give an overview of recent measurements of top-antitop differential cross sections and charge asymmetry in p-p collisions. Recent results and their comparison with SM predictions will be presented. The talk will focus on ongoing studies of a new measurement of the top-antitop charge asymmetry at the ATLAS experiment. Event reconstruction and detector effects will be discussed. In addition, a method to generate top-antitop events at the NNLO QCD precision, MiNNLOPS, is presented. Validation studies of the MiNNLOPS framework are conducted by comparing kinematic distributions and checking the consistency of the samples. These studies aim to check the reliability of the method for precision measurements in top-quark physics.

Infrared Finiteness in Flavor-violating Scattering Processes of Axion Production

Matak P. and Sinska Z.

Abstract. In decays and scatterings of heavy quarks in the early universe, axion-like particles as dark matter candidates can be produced through a freeze-in mechanism. Within this framework, infrared divergences arise in the calculation of the axion production rates. We show how an approach based on holomorphic cutting rules and the Kinoshita-Lee-Nauenberg theorem can be applied to identify the relevant contributions required to ensure infrared finiteness.

F-12 PHYSICS EDUCATION AND GENERAL PROBLEMS OF PHYSICS

Adaptation of the Quantum Mechanics Concept Assessment into Czech

Kafka J.

Abstract. This contribution presents preliminary results of a pilot study conducted as the final stage of the adaptation of the Quantum Mechanics Concept Assessment (QMCA) into the Czech language. The study involved undergraduate physics students and pre-service physics teachers enrolled in introductory quantum mechanics courses. Among other aspects, it investigates how students understand selected fundamental concepts in quantum mechanics and examines the performance of the Czech version of the instrument.

Out-of-field Teaching

Kohout V.

Abstract. The aim of my future dissertation is to explore out-of-field physics teaching in the Czech Republic. This literature review summarizes worldwide studies on out-of-field teaching, focusing on its definitions, occurrence, causes, teachers' experiences, and impact on students. The review also identifies factors influencing teachers' adaptation to out-of-field teaching. Finally, we present key topics for a questionnaire that will be developed for Czech physics teachers.

Exploring Barriers and Opportunities for Mobile Device Use in Czech Physics Teaching

Nauš J.

Abstract. This study examines perceived barriers and opportunities for mobile device use in Czech physics teaching. It is based on a 2025 online survey of Czech physics teachers (N=337) combining Likert-type items and open-ended responses. It asks what barriers and opportunities teachers report and how these relate to device type, teaching experience, and other relevant factors.



F-13 PHYSICS OF NANOSTRUCTURES AND NANOMATERIALS

DFT Calculations of Magnetic Structure in Cu₂Sb-type Materials

Parizek V.

Abstract. Antiferromagnets such as CuMnAs and Mn₂As are promising for spintronics due to fast dynamics, zero stray fields, and current-induced switching. These compounds, part of the Cu₂Sb-type family, exhibit complex magnetic behavior and long-lived metastable states, but their microscopic mechanisms remain unclear. We calculate their structural and magnetic properties. We use Density functional theory to obtain the lattice parameters and atomic positions. This is then used to obtain the ground state magnetic structure of a material.

Temperature-Dependent Raman Spectroscopy of KTa_{1-x}Nb_xO₃ Single Crystals

Pescaru C. A., Borodavka F., Savinov M., and Hlinka J.

Abstract. KTa_{1-x}Nb_xO₃ (KTN) single crystals are promising perovskite materials due to their tunable dielectric and ferroelectric properties. Their complex structural behavior and temperature-dependent phase transitions motivate further investigation using complementary experimental techniques. In this work, dielectric and Raman spectroscopic methods were combined to study the vibrational and structural properties of KTN single crystals. Dielectric measurements revealed temperature-dependent variations in the dielectric response near room temperature, motivating further investigation by polarized Raman spectroscopy. Raman measurements were performed between 300 and 4 K using a 514 nm excitation source. The obtained spectra show temperature-dependent changes associated with structural phase transitions of the perovskite lattice. This ongoing work aims to contribute to a better understanding of the relationship between dielectric behavior and lattice dynamics in KTN materials.



